Unitarity corrections to $K^+ \to \pi^+ \gamma l^+ l^-$

Fabrizio Gabbiani

Department of Physics

Duke University, Durham, North Carolina 27708

Abstract

We perform a chiral one-loop calculation of the unitarity corrections to the processes $K^+ \to \pi^+ \gamma l^+ l^-$ up to $\mathcal{O}(\mathrm{E}^6)$, taking into account $\pi^+ \pi^-$ intermediate states. Branching ratios and differential branching ratios are computed and presented to demonstrate the importance of the above corrections.

I. Introduction

The investigation of radiative rare kaon decays has taught us that they form a complex of interrelated processes which share some common features. Experimental and theoretical results on any of these reactions are useful in the analysis of all of them. Since they can be analyzed using chiral perturbation theory (ChPT) [1], the experimental exploration of the entire complex provides stringent checks on this theoretical method. Recently, radiative kaon decays have attracted considerable attention from the theoretical [2, 3, 4, 5] and the experimental [6, 7] communities. Predictions for many of them already exist in the literature [8, 9, 10, 11, 12, 13, 14], and several new experimental investigations are under way or planned. In particular, initial data on the process $K_L \to \pi^0 \gamma e^+ e^-$ [3] have already been presented [7], together with further data on $K_L \to \pi^0 \gamma \gamma$. Confident that the objects of our calculation, the decays $K^+ \to \pi^+ \gamma l^+ l^-$, are accessible to experiment, our goal is to provide information on their rate and the corresponding decay distributions.

Analogously to what has been studied in the case of $K_L \to \pi^0 \gamma \gamma$, the reaction $K^+ \to \pi^+ \gamma \gamma$ takes place predominantly through loop diagrams with pions in the loop. In the former process, the decay distribution is quite distinctive and the rate is predicted without any free parameters at one-loop order. While the distribution agrees well with experiment, the theoretical rate appears too small by more than a factor of 2. Because of this, several authors have gone beyond the straightforward one-loop (order E^4) chiral calculation. Adding a series of higher order effects in a quasi-dispersive framework one has a surprising success at increasing the rate without modifying the decay distribution greatly [10, 9]. The process $K^+ \to \pi^+ \gamma \gamma$ has been studied in a similar way [12, 13]. The physics which determines the above decays is also involved in the reaction we consider. The experimental study of the lepton-photon modes can achieve independent confirmation of the dynamics that drives the whole complex of decay modes.

As was done in previous works, we separately calculate the one-loop results within ChPT both at $\mathcal{O}(\mathrm{E}^4)$ and $\mathcal{O}(\mathrm{E}^6)$. The first one gives a prediction for the rate and the variation of the amplitude depending on the invariant mass of the two leptons, k_1^2, which is carried by an off-shell photon. An additional parameter, in the form of a local counterterm, also enters the calculation. In the second case, following Ref. [12], we take into account the higher order behavior in the experimental $K^+ \to 3\pi$ decay rate.

At $\mathcal{O}(\mathrm{E}^6)$ the higher order effects in the $K^+ \to 3\pi$ vertex are extracted from a quadratic fit to the amplitude. According to the results of Refs. [12, 13], we shall not be concerned with vector meson corrections, likely too small to be significant, given the uncertainties in the several parameters involved in this computation.

This paper is organized as follows: In Sec. II we fix our notation and define the quantities used in the rest of this paper by summarizing some established results for the decay $K^+ \to \pi^+\gamma\gamma$. This provides a starting point for our calculation, taking a photon off shell and going through the process $K^+ \to \pi^+\gamma\gamma^* \to \pi^+\gamma l^+ l^-$. In Sec. III we describe the $\mathcal{O}(E^4)$ calculation, which we extend to $\mathcal{O}(E^6)$ in Sec. IV, taking into account the unitarity corrections at one loop. Finally, we recapitulate our conclusions in Sec. V. All the relevant expressions for the integrals used in this paper are shown in the Appendix.

II. $K \to \pi\gamma\gamma$ amplitudes

Let us first review some previously known results for $K \to \pi\gamma\gamma$, and establish our notation for the following sections. We define the general amplitude for $K \to \pi\gamma\gamma$ as given by

$$M[K(p_K) \to \pi(p)\gamma(k_1, \epsilon_1)\gamma(k_2, \epsilon_2)] = \epsilon_{1\mu}\epsilon_{2\nu}\mathcal{M}^{\mu\nu}(p_K, k_1, k_2) \tag{1}$$

where ϵ_1, ϵ_2 are the photon polarizations, and $\mathcal{M}^{\mu\nu}$ has four invariant amplitudes:

$$
\begin{aligned}
\mathcal{M}^{\mu\nu} &= A(z,y)(k_2^\mu k_1^\nu - k_1 \cdot k_2 g^{\mu\nu}) \\
&+ B(z,y)\left(\frac{p_K \cdot k_1 p \cdot k_2}{k_1 \cdot k_2}g^{\mu\nu} + p_K^\mu p_K^\nu - \frac{p_K \cdot k_1}{k_1 \cdot k_2}k_2^\mu p_K^\nu - \frac{p_K \cdot k_2}{k_1 \cdot k_2}p_K^\mu k_1^\nu\right) \\
&+ C_1(z,y)\varepsilon^{\mu\nu\rho\sigma}k_{1\rho}k_{2\sigma} \\
&+ C_2(z,y)\left[\varepsilon^{\mu\nu\rho\sigma}\frac{p_K \cdot k_2 k_{1\rho} + p_K \cdot k_1 k_{2\rho}}{k_1 \cdot k_2}p_{K\sigma} + (p_K^\mu \varepsilon^{\nu\alpha\beta\gamma} + p_K^\nu \varepsilon^{\mu\alpha\beta\gamma})p_{K\alpha}\frac{k_{1\beta}k_{2\gamma}}{k_1 \cdot k_2}\right]
\end{aligned}
\tag{2}
$$

where

$$y = \frac{p_K \cdot (k_1 - k_2)}{m_K^2}, \qquad z = \frac{(k_1 + k_2)^2}{m_K^2}. \tag{3}$$

The physical region in the adimensional variables y and z is given by

$$0 \le |y| \le \frac{1}{2}\lambda^{1/2}(1, r_\pi^2, z), \qquad 0 \le z \le (1 - r_\pi)^2, \tag{4}$$

with

$$\lambda(1, z, r^2) = 1 + z^2 + r^4 - 2z - 2r^2 - 2r^2 z, \qquad r_\pi = \frac{m_\pi}{m_K}. \tag{5}$$

Here k_1 and k_2 are the momenta of the off-shell and on-shell photons, respectively, with the off-shell photon materializing into the lepton pair. Note that the invariant amplitudes $A(z,y)$, $B(z,y)$ and $C_1(z,y)$ have to be symmetric under the interchange of k_1 and k_2 as required by Bose symmetry, while $C_2(z,y)$ is antisymmetric.

Using the definitions (2)–(5) the double differential rate for unpolarized photons is given by

$$
\begin{aligned}
\frac{d^2\Gamma}{dydz} &= \frac{m_K^5}{2^9\pi^3}\left\{z^2\left(\left|A - \frac{B}{2}\right|^2 + |C_1|^2\right)\right. \\
&+ \left.\left[y^2 - \frac{1}{4}\lambda(1, r_\pi^2, z)\right]^2\left(\frac{|B|^2}{4} + |C_2|^2\right)\right\}.
\end{aligned}
\tag{6}
$$

In the limit where CP is conserved, the amplitudes A and B contribute to $K_2 \to \pi^0\gamma\gamma$ whereas $K_1 \to \pi^0\gamma\gamma$ involves the other two amplitudes C_1 and C_2. All four amplitudes contribute to $K^+ \to \pi^+\gamma\gamma$. Only A and

C_1 are non-vanishing to lowest non-trivial order, $\mathcal{O}(E^4)$, in ChPT. As argued in [15, 12], the antisymmetric character of the $C_2(z,y)$ amplitude under the interchange of k_1 and k_2 means effectively that while its leading contribution is $\mathcal{O}(E^6)$, this can only come from a finite loop calculation because the leading counterterms for the C_2 amplitude are $\mathcal{O}(E^8)$. Moreover, this loop contribution is helicity suppressed compared to the B term. This antisymmetric $\mathcal{O}(E^6)$ loop contribution might be smaller than the local $\mathcal{O}(E^8)$ contribution.

III. $\mathcal{O}(\text{E}^4)$ calculation

First let us provide the straightforward $\mathcal{O}(E^4)$ calculation of $\mathcal{M}(K^+ \to \pi^+\gamma l^+ l^-)$ within ChPT. This is the generalization to $k_1^2 \neq 0$ of the original chiral calculation of the authors of [16, 17], and it includes all the k_1^2/m_π^2 and $q \equiv k_1^2/m_K^2$ variations of the amplitudes at this order in the energy expansion. There can be further $k_1^2/(1\text{ GeV})^2$ corrections which correspond to $\mathcal{O}(E^6)$ and higher. The easiest technique for this calculation uses the basis where the kaon and pion fields are transformed so that the propagators have no off-diagonal terms, as described in Refs. [16, 17]. Some of the relevant diagrams are shown in Fig. 1.
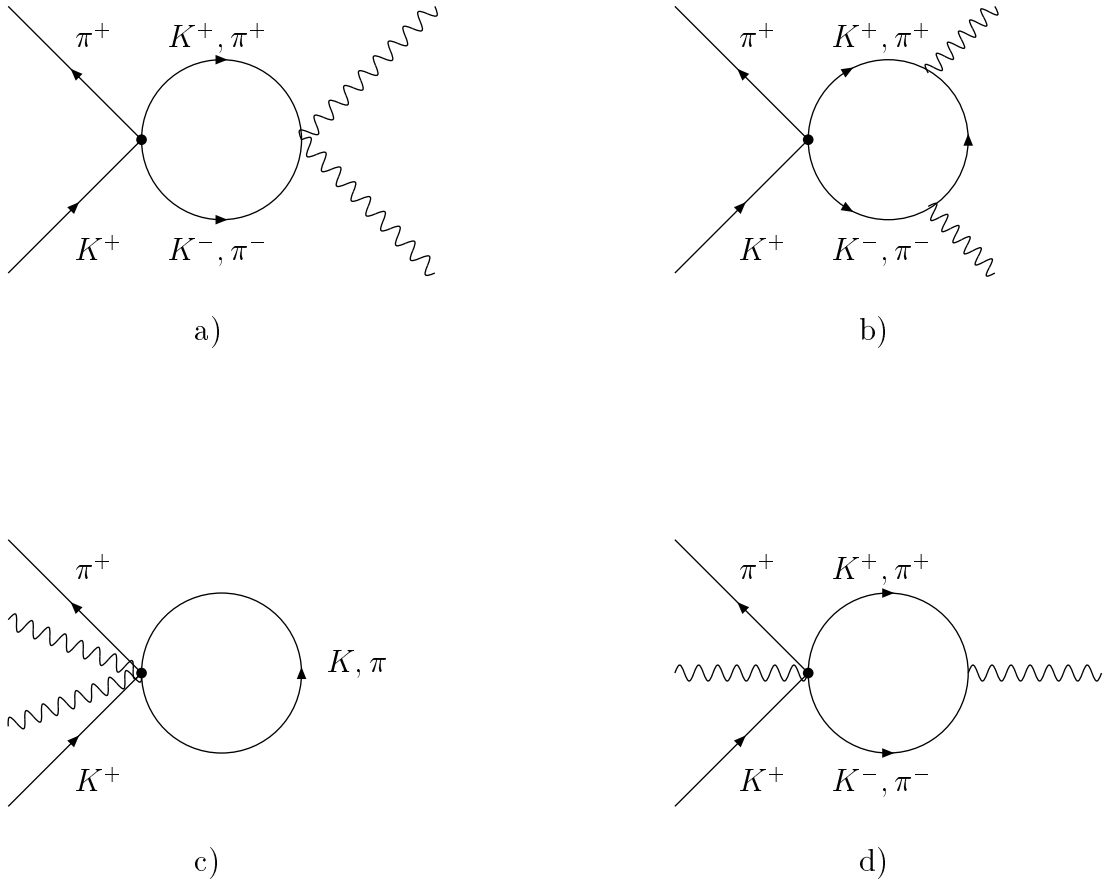

Figure 1: Some diagrams relevant to the process $K^+ \to \pi^+\gamma l^+ l^-$ at $\mathcal{O}(E^4)$ and $\mathcal{O}(E^6)$. Either photon may also be radiated from the incoming K^+ or the outcoming π^+. The lepton pair must be attached to one of the photons, and the on-shell photon may be radiated from one of these leptons.

Analogously to the leading $\Delta I = 1/2$ $\mathcal{O}(E^4)$ $A(z,y)$ and $C_1(z,y)$ amplitudes for $K^+ \to \pi^+\gamma\gamma$ which have been computed in [17], we can write an expression for the $A^{(4)}$ amplitude for $K^+ \to \pi^+\gamma\gamma^*$,

$$A^{(4)}(z) = \frac{G_8\alpha_{em}}{2\pi(z-q)}\left\{(z+1-r_\pi^2)[1+2I(m_\pi^2)] + (z+r_\pi^2-1)[1+2I(m_K^2)] - \hat{c}(z-q)\right\}, \qquad (7)$$

3

where G_8 is the effective weak coupling constant determined from $K \to \pi\pi$ decays at $\mathcal{O}(E^2)$:

$$\begin{aligned} G_8 &= \frac{G_F}{\sqrt{2}}|V_{ud}V_{us}^*|g_8, \\ g_8^{\text{tree}} &= 5.1, \end{aligned} \tag{8}$$

where V is the Cabibbo-Kobayashi-Maskawa matrix [18], and

$$\begin{aligned} I(m_\pi^2) &= \int_0^1 dz_1 \int_0^{1-z_1} dz_2 \frac{m_\pi^2 - z_1(1-z_1)k_1^2}{2z_1z_2k_1 \cdot k_2 + z_1(1-z_1)k_1^2 - m_\pi^2 + i\epsilon} \\ &= \frac{m_\pi^2}{s - k_1^2}[F(s) - F(k_1^2)] - \frac{k_1^2}{s - k_1^2}[G(s) - G(k_1^2)]. \end{aligned} \tag{9}$$

The notation is defined by

$$s = (p_K - p_+)^2 = (k_1 + k_2)^2 \tag{10}$$

and

$$F(a) = \int_0^1 \frac{dz_1}{z_1} \log\left[\frac{m_\pi^2 - a(1-z_1)z_1 - i\epsilon}{m_\pi^2}\right], \tag{11}$$

$$G(a) = \int_0^1 dz_1 \log\left[\frac{m_\pi^2 - a(1-z_1)z_1 - i\epsilon}{m_\pi^2}\right]. \tag{12}$$

The above functions are related to those presented in Ref. [9],

$$F(a) = \frac{a}{2m_\pi^2}\left[F_{\text{CEP}}\left(\frac{a}{4m_\pi^2}\right) - 1\right], \tag{13}$$

$$G(a) = -\frac{a}{2m_\pi^2}\left[R_{\text{CEP}}\left(\frac{a}{4m_\pi^2}\right) + \frac{1}{6}\right], \tag{14}$$

which are shown below:

$$\begin{aligned} F_{\text{CEP}}(x) &= 1 - \frac{1}{x}\left[\arcsin\left(\sqrt{x}\right)\right]^2 \qquad (x \leq 1) \\ &= 1 + \frac{1}{4x}\left(\log\frac{1 - \sqrt{1 - 1/x}}{1 + \sqrt{1 - 1/x}} + i\pi\right)^2 \qquad (x \geq 1), \end{aligned} \tag{15}$$

$$\begin{aligned} R_{\text{CEP}}(x) &= -\frac{1}{6} + \frac{1}{2x}\left[1 - \sqrt{1/x - 1}\arcsin\left(\sqrt{x}\right)\right] \qquad (x \leq 1) \\ &\quad -\frac{1}{6} + \frac{1}{2x}\left[1 + \sqrt{1 - 1/x}\left(\log\frac{1 - \sqrt{1 - 1/x}}{1 + \sqrt{1 - 1/x}} + i\pi\right)\right], \qquad (x \geq 1). \end{aligned} \tag{16}$$

The above results agree with the results obtained in [12] in the $k_1^2 \to 0$ limit.

In Eq. (7) the pion loop contribution largely dominates over the kaon loop part. The loop results are finite, but ChPT allows an $\mathcal{O}(E^4)$ scale independent local contribution that may be parametrized as [19]

$$\hat{c} = \frac{128\pi^2}{3}[3(L_9 + L_{10}) + N_{14} - N_{15} - 2N_{18}] \tag{17}$$

or, using the notation of [17, 20],

$$\hat{c} = \frac{32\pi^2}{3}[12(L_9 + L_{10}) - w_1 - 2w_2 - 2w_4], \tag{18}$$

where $\hat{c}$ is a quantity of $\mathcal{O}(1)$. The L_9 and L_{10} are the local $\mathcal{O}(\mathrm{E}^4)$ strong couplings and N_{14}, N_{15} and N_{18} (or w_1, w_2 and w_4) are $\mathcal{O}(\mathrm{E}^4)$ weak couplings, still not completely fixed by the phenomenology, and which can be only computed in a model dependent way [21]. The weak deformation model (WDM) [20] predicts $\hat{c} = 0$, while naive factorization in the factorization model (FM) [22, 21] gives $\hat{c} = -2.3$. In these models, because of the cancellation in the vector meson contribution in $\hat{c}$, the role of axial mesons could be relevant [21].

Thirty-one events for the process $K^+ \to \pi^+\gamma\gamma$ have been observed at BNL (E787) [23], with the partial branching ratio $\mathrm{BR}(K^+ \to \pi^+\gamma\gamma, 100\,\mathrm{MeV}/c < P_{\pi^+} < 180\,\mathrm{MeV}/c) = (6.0\pm1.5\{\mathrm{stat}\}\pm0.7\{\mathrm{syst}\})\times10^{-7}$. This has been extrapolated with the help of ChPT, performing a maximum likelihood fit of $\hat{c}$ to the spectrum. The results of the fit to the data support the inclusion of the unitarity corrections, giving as the best fit $\hat{c} = 1.8 \pm 0.6$ and $\mathrm{BR}(K^+ \to \pi^+\gamma\gamma) = (1.1 \pm 0.3 \pm 0.1) \times 10^{-6}$, as also reported in the Review of Particle Physics [24].

The $\mathcal{O}(\mathrm{E}^4)$ contribution to the $C_1(z, y)$ amplitude is

$$C_1(z) = \frac{G_8\alpha_{em}}{\pi}\left[\frac{z - r_\pi^2}{z - r_\pi^2 + ir_\pi\dfrac{\Gamma_{\pi^0}}{m_K}} - \frac{z - \dfrac{2 + r_\pi^2}{3}}{z - r_\eta^2}\right], \tag{19}$$

where $r_\eta = m_\eta/m_K$ and $\Gamma_{\pi^0} \equiv \Gamma(\pi^0 \to \gamma\gamma^*) \sim 0$. This amplitude is generated by the Wess–Zumino–Witten functional [25] $(\pi^0, \eta) \to \gamma\gamma^*$ through the sequence $K^+ \to \pi^+(\pi^0, \eta) \to \pi^+\gamma\gamma^*$. This contribution amounts to less than 10% in the total width.

The $\mathcal{O}(\mathrm{E}^4)$ results can be expressed as total branching ratios. They are summarized in Table I for three values of $\hat{c}$, given respectively by the weak deformation model, the factorization model, and the fit to $\mathrm{BR}(K^+ \to \pi^+\gamma\gamma)$ mentioned above.

Table 1: Results for $\mathrm{BR}(K^+ \to \pi^+\gamma l^+l^-)$ at $\mathcal{O}(\mathrm{E}^4)$.

	$\mathrm{BR}(K^+ \to \pi^+\gamma e^+e^-)$	$\mathrm{BR}(K^+ \to \pi^+\gamma\mu^+\mu^-)$
$\hat{c} = 1.8$ (fit)	1.4×10^{-8}	3.9×10^{-11}
$\hat{c} = 0$ (WDM)	8.6×10^{-9}	3.6×10^{-11}
$\hat{c} = -2.3$ (FM)	5.7×10^{-9}	3.9×10^{-11}

The decay distributions in z and y provide more detailed information. We present them in Figs. 2–5.

IV. $\mathcal{O}(\mathrm{E}^6)$ calculation

In this section we extend this calculation along the lines proposed by the authors of Refs. [9, 10] for K_L decays and D'Ambrosio and Portolés for K^+ decays [12]. The former provided a plausible solution to the problem raised by the experimental rate not agreeing with the $\mathcal{O}(\mathrm{E}^4)$ calculation when both photons are on shell. We have to add a new ingredient that involves known physics that surfaces at the next order in
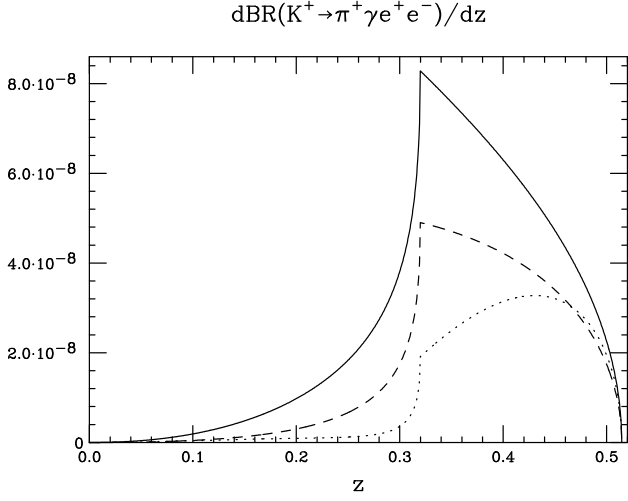
$$\mathrm{dBR(K^+ \to \pi^+ \gamma e^+ e^-)/dz}$$

Figure 2: The differential branching ratio $\mathrm{dBR}(K^+ \to \pi^+\gamma e^+ e^-)/dz$ to order E^4 is plotted vs z for $\hat{c} = 1.8$ (solid line), $\hat{c} = 0$ (dashed line) and $\hat{c} = -2.3$ (dotted line).
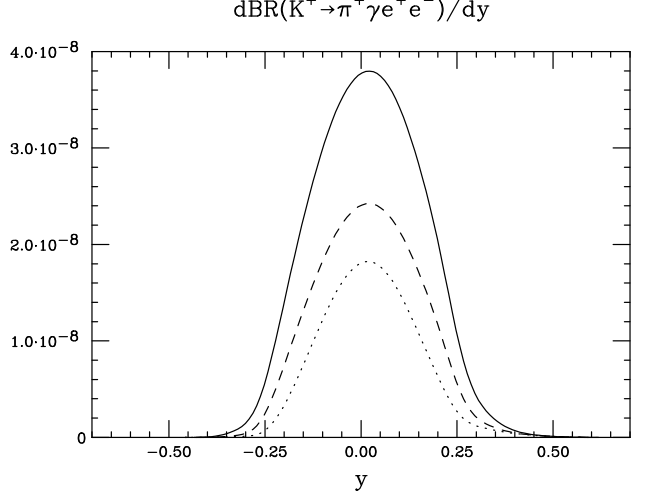

$$\mathrm{dBR(K^+ \to \pi^+ \gamma e^+ e^-)/dy}$$

Figure 3: The differential branching ratio $\mathrm{dBR}(K^+ \to \pi^+\gamma e^+ e^-)/dy$ to order E^4 is plotted vs y for $\hat{c} = 1.8$ (solid line), $\hat{c} = 0$ (dashed line) and $\hat{c} = -2.3$ (dotted line).
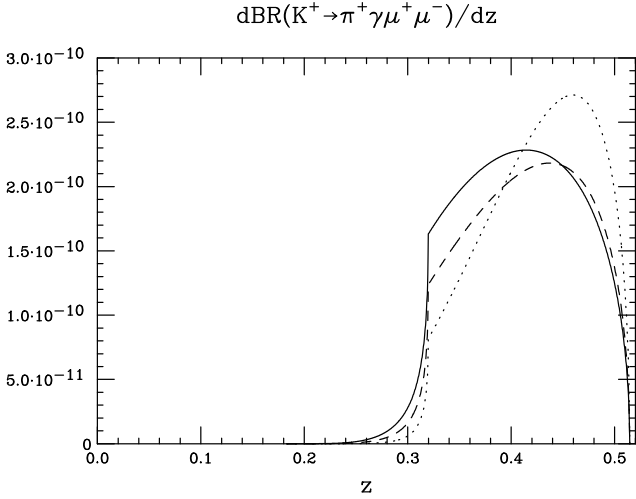

$$\mathrm{dBR(K^+ \to \pi^+ \gamma \mu^+ \mu^-)/dz}$$

Figure 4: The differential branching ratio $\mathrm{dBR}(K^+ \to \pi^+\gamma\mu^+\mu^-)/dz$ to order E^4 is plotted vs z for $\hat{c} = 1.8$ (solid line), $\hat{c} = 0$ (dashed line) and $\hat{c} = -2.3$ (dotted line).
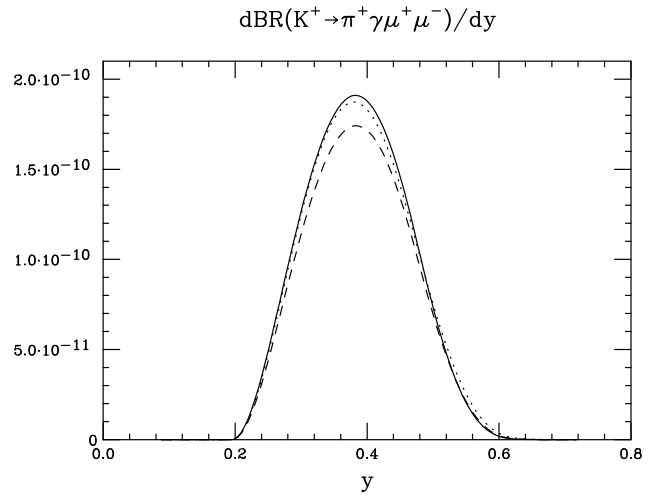

$$\mathrm{dBR(K^+ \to \pi^+ \gamma \mu^+ \mu^-)/dy}$$

Figure 5: The differential branching ratio $\mathrm{dBR}(K^+ \to \pi^+\gamma\mu^+\mu^-)/dy$ to order E^4 is plotted vs y for $\hat{c} = 1.8$ (solid line), $\hat{c} = 0$ (dashed line) and $\hat{c} = -2.3$ (dotted line).

the energy expansion, i.e. the known quadratic energy variation of the $K \to 3\pi$ amplitude, which occurs from higher order terms in the weak nonleptonic Lagrangian [26, 10, 2, 27]. While the full one-loop structure of this is known [19, 28, 29], it involves complicated nonanalytic functions and we approximate the result at $\mathcal{O}(\mathrm{E}^4)$ by an analytic polynomial which provides a good description of the data throughout the physical region [30, 28]. Expanding in powers of the Dalitz plot variables,

$$
\begin{aligned}
A^{(4)}(K^+ \to \pi^+ \pi^+ \pi^-) &= 2\alpha_1 - \alpha_3 + \left(\beta_1 - \frac{1}{2}\beta_3 + \sqrt{3}\gamma_3\right) Y \\
&\quad - 2(\zeta_1 + \zeta_3)\left(Y^2 + \frac{X^2}{3}\right) - (\xi_1 + \xi_3 - \xi_3')\left(Y^2 - \frac{X^2}{3}\right).
\end{aligned}
\tag{20}
$$

Here the subscripts 1 and 3 refer to $\Delta I = 1/2, 3/2$ transitions respectively, and the coefficients in Eq. (20) have been fitted to the data [28]. We omit the $\Delta I = 3/2$ couplings ζ_3 and ξ_3, ξ_3' because of their big errors shown in the fits in Ref. [28]. The Dalitz plot variables are commonly defined as

$$
X = \frac{s_2 - s_1}{m_\pi^2}, \qquad Y = \frac{s_3 - s_0}{m_\pi^2},
\tag{21}
$$

with $s_i = (p_K - p_i)^2$ for $i = 1, 2, 3$, $s_0 = (s_1 + s_2 + s_3)/3$, and the subscript 3 indicates the odd pion (π^0 for K_L decays and π^- for K^+ decays).

In principle one can add the ingredients to the amplitudes and perform a dispersive calculation of the total transition matrix element. In practice it is simpler to convert the problem into an effective field theory and and do a Feynman-diagram calculation which will yield the same result. We follow this latter procedure.

The Feynman diagrams are the same as shown in Fig. 1, although the vertices are modified by the presence of $\mathcal{O}(\mathrm{E}^4)$ terms in the energy expansion. Not only does the direct $K \to 3\pi$ vertex change to the form given in Eq. (20), but also the weak vertices with one and two photons have a related change. The easiest way to determine these is to write a gauge invariant effective Lagrangian with coefficients adjusted to reproduce Eq. (20). One also has to add diagrams with one or two photons radiating from the incoming K^+ or the outcoming π^+, or with one photon radiating from one of the outcoming leptons. This causes infrared divergences, which are to be treated in the usual way, as part of a general calculation of radiative corrections to the process $K^+ \to \pi^+ l^+ l^-$. In practice, with an appropriate set of experimental cuts on the phase space parameters, it is possible to restrict the outcome to a measurable non-bremsstrahlung contribution only [31]. Below we shall give an example of these cuts and a prediction for the experimental result once they are implemented.

The resulting calculation follows the same steps as described in Sec. III, but is more involved and is not easy to present in a simple form. We have checked that our result reduces to that of Ref. [12] in the limit of on-shell photons. Remembering the definitions

$$
r_\pi = \frac{m_\pi}{m_K}, \qquad r_\eta = \frac{m_\eta}{m_K}, \qquad z = \frac{s}{m_K^2}, \qquad q = \frac{k_1^2}{m_K^2},
\tag{22}
$$

the unitarity one-loop corrections yield the following:

$$
\begin{aligned}
\mathcal{M}_{\mu\nu} &= \frac{\alpha_{em}}{2\pi}\Bigg[A(z, y, q)(k_{2\mu}k_{1\nu} - k_1 \cdot k_2 g_{\mu\nu}) \\
&\quad + B(z, y, q)\left(\frac{p_K \cdot k_1 p_K \cdot k_2}{k_1 \cdot k_2}g_{\mu\nu} + p_{K\mu}p_{K\nu} - \frac{p_K \cdot k_1}{k_1 \cdot k_2}k_{2\mu}p_{K\nu} - \frac{p_K \cdot k_2}{k_1 \cdot k_2}k_{1\nu}p_{K\mu}\right) \\
&\quad + C_1(z)\varepsilon_{\mu\nu\rho\sigma}k_1{}^\rho k_2{}^\sigma
\end{aligned}
$$

$$+ \ D(z,y,q) \left(k_1^2 \frac{p_K \cdot k_2}{k_1 \cdot k_2} g_{\mu\nu} - \frac{p_K \cdot k_2}{k_1 \cdot k_2} k_{1\mu} k_{1\nu} + k_{1\mu} p_{K\nu} - \frac{k_1^2}{k_1 \cdot k_2} k_{2\mu} p_{K\nu} \right) \Bigg] ,$$

(23)

where

$$
\begin{aligned}
Am_K^2 \ = \ & \frac{G_8 m_K^2}{(z-q)} \{ (z + r_\pi^2 - 1)[1 + 2I(m_K^2)] - \hat{c}(z-q) \} \\
+ \ & \left\{ 2(2\alpha_1 - \alpha_3) + \left(1 + \frac{1}{3r_\pi^2} - \frac{z}{r_\pi^2} \right) \left(\beta_1 - \frac{1}{2}\beta_3 + \sqrt{3}\gamma_3 \right) \right. \\
- \ & \frac{8}{3r_\pi^4}(2\zeta_1 - \xi_1)\frac{1}{18}\left[1 + 6(r_\pi^2 - z) + 9(r_\pi^2 - z)^2 \right] \Bigg\} [1 + 2I(m_\pi^2)] \\
- \ & \frac{8}{3r_\pi^4}(2\zeta_1 - \xi_1)\left[\left(r_\pi^2 - \frac{q}{12} \right) \log \frac{m_\pi^2}{\mu^2} + \frac{1}{2}I_4 \right] \\
- \ & \frac{8}{3r_\pi^4}(4\zeta_1 + \xi_1) \left\{ - \{ 2[1 - 2(x_1 + x_2)]I_1(z_1 z_2) + x_1 I_1(z_2) \right. \\
+ \ & x_2[2I_1(z_2^2) - I_1(z_2) + I_1(z_1)] \} \\
+ \ & 2\{ [2x_1^2 - x_1(z+q)][-I_2(z_1^3 z_2) + I_2(z_1^2 z_2)] \\
+ \ & [2x_1 x_2 - x_1(z-q)/2 - x_2(z+q)/2][2I_2(z_1^2 z_2^2) + I_2(z_1 z_2) - I_2(z_1^2 z_2) \\
- \ & I_2(z_1 z_2^2)] + [2x_2^2 - x_2(z-q)][I_2(z_1 z_2^2) - I_2(z_1 z_2^3)] \} \\
+ \ & \left[\frac{1}{9}(1 - 3r_\pi^2) + \frac{1}{12}r_\pi^2(1 + 3r_\pi^2)\left(1 + \frac{1}{3r_\pi^2} - \frac{z}{r_\pi^2} \right) \right] [1 + 2I(m_\pi^2)] \\
- \ & \frac{1}{12}\left(1 + \log \frac{m_\pi^2}{\mu^2} \right) - \frac{1}{2}\left(r_\pi^2 - \frac{q}{12} \right) \log \frac{m_\pi^2}{\mu^2} - \frac{1}{4}I_4 \Bigg\} ,
\end{aligned}
$$

(24)

$$
\begin{aligned}
Bm_K^2 \ = \ & \frac{8}{3r_\pi^4}(4\zeta_1 + \xi_1) \left\{ -2I_3 + I_4 + \frac{1}{12}(z-q)\log \frac{m_\pi^2}{\mu^2} \right. \\
- \ & \frac{1}{4}\left(\frac{q}{6}\log \frac{m_\pi^2}{\mu^2} - I_4 \right) \Bigg\} ,
\end{aligned}
$$

(25)

$$C_1 m_K^2 = 2G_8 m_K^2 \frac{2 + r_\pi^2 - 3r_\eta^2}{3(z - r_\pi^2)},$$

(26)

$$
\begin{aligned}
Dm_K^2 \ = \ & \frac{8}{3r_\pi^4}(4\zeta_1 + \xi_1) \left\{ I_3 - \frac{I_4}{2} - \frac{1}{24}(z-q)\log \frac{m_\pi^2}{\mu^2} \right. \\
+ \ & [2x_2 - (z-q)/2][2I_1(z_1 z_2) - I_1(z_2)] \\
+ \ & (2y - q)[I_1(z_1) - I_1(1)/2] + [2x_1 - (z+q)/2]\frac{I_5}{4} \Bigg\} .
\end{aligned}
$$

(27)

The integrals used in the above formulas are defined here and given explicitly in the Appendix:

$$I_1(z_1^n z_2^m) = \int_0^1 dz_1 \int_0^{1-z_1} dz_2 z_1^n z_2^m \log \frac{D_1}{m_\pi^2},$$

(28)

$$\frac{I_2(z_1^n z_2^m)}{m_K^2} = \int_0^1 dz_1 \int_0^{1-z_1} dz_2 \frac{z_1^n z_2^m}{D_1}, \tag{29}$$

$$I_3 m_K^2 = \int_0^1 dz_1 \int_0^{1-z_1} dz_2 D_1 \log \frac{D_1}{m_\pi^2}, \tag{30}$$

$$I_4 m_K^2 = \int_0^1 dz_1 D_2 \log \frac{D_2}{m_\pi^2}, \tag{31}$$

$$I_5 = \int_0^1 dz_1 (4z_1^2 - 4z_1 + 1) \log \frac{D_2}{m_\pi^2}, \tag{32}$$

where

$$\begin{aligned}
D_1 &= m_\pi^2 - 2k_1 \cdot k_2 z_1 z_2 - k_1^2 z_1 (1 - z_1), \\
D_2 &= m_\pi^2 - k_1^2 z_1 (1 - z_1), \\
x_1 &= \frac{p_K \cdot k_1}{m_K^2}, \qquad x_2 = \frac{p_K \cdot k_2}{m_K^2}.
\end{aligned} \tag{33}$$

The above formulas lead to the total branching ratios shown in Table II, in full analogy with the results of Sec. III. The numerical results are obtained for the mass scale $\mu = m_\rho$ and setting all the counterterms to 0 [12]. The corresponding decay distributions are plotted in Figs. 6–9.

Table 2: Results for $\mathrm{BR}(K^+ \to \pi^+ \gamma l^+ l^-)$ at $\mathcal{O}(\mathrm{E}^6)$.

	$\mathrm{BR}(K^+ \to \pi^+ \gamma e^+ e^-)$	$\mathrm{BR}(K^+ \to \pi^+ \gamma \mu^+ \mu^-)$
$\hat{c} = 1.8$ (fit)	1.7×10^{-8}	7.0×10^{-11}
$\hat{c} = 0$ (WDM)	1.1×10^{-8}	7.3×10^{-11}
$\hat{c} = -2.3$ (FM)	9.2×10^{-9}	8.5×10^{-11}

The uncertainty in the theoretical prediction is dominated by the unknown $\mathcal{O}(\mathrm{E}^4)$ counterterm generated amplitude $\hat{c}$ in Eq. (7). In Figs. 10 and 11 we plot $\mathrm{BR}(K^+ \to \pi^+ \gamma e^+ e^-)$ and $\mathrm{BR}(K^+ \to \pi^+ \gamma \mu^+ \mu^-)$ as a function of $\hat{c}$, both with and without the $\mathcal{O}(\mathrm{E}^6)$ corrections just computed.

If we implement the experimental cuts currently used at BNL to extract the non-bremsstrahlung contribution to $K^+ \to \pi^+ \gamma e^+ e^-$ [31],

$$m_{e^+e^-} \geq 150 \text{ MeV}, \quad E_\gamma \geq 30 \text{ MeV}, \quad m_{e^+\gamma}, m_{e^-\gamma} \geq 30 \text{ MeV}, \tag{34}$$

the resulting theoretical branching ratios are reduced by more than an order of magnitude. They are presented in Table III. Preliminary experimental data are not conclusive at the present stage. In Figs. 12 and 13 we plot the differential branching ratios up to $\mathcal{O}(\mathrm{E}^6)$, taking into account the above cuts in the phase space integration.
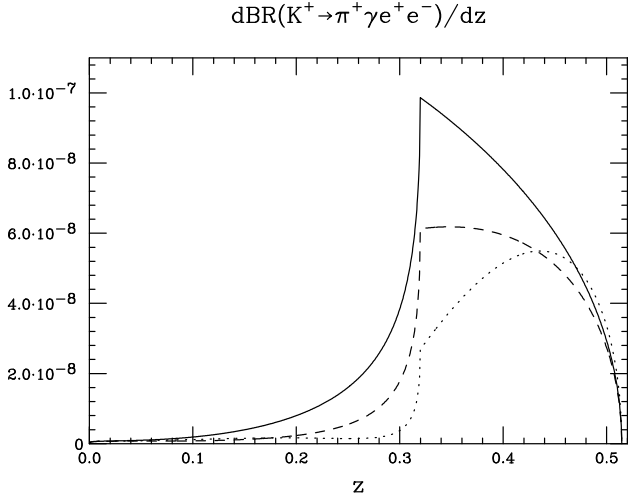
dBR(K⁺→π⁺γe⁺e⁻)/dz

dBR(K⁺→π⁺γe⁺e⁻)/dy

Figure 6: The differential branching ratio $dBR(K^+ \to \pi^+\gamma e^+e^-)/dz$ to order E^6 is plotted vs z for $\hat{c} = 1.8$ (solid line), $\hat{c} = 0$ (dashed line) and $\hat{c} = -2.3$ (dotted line).
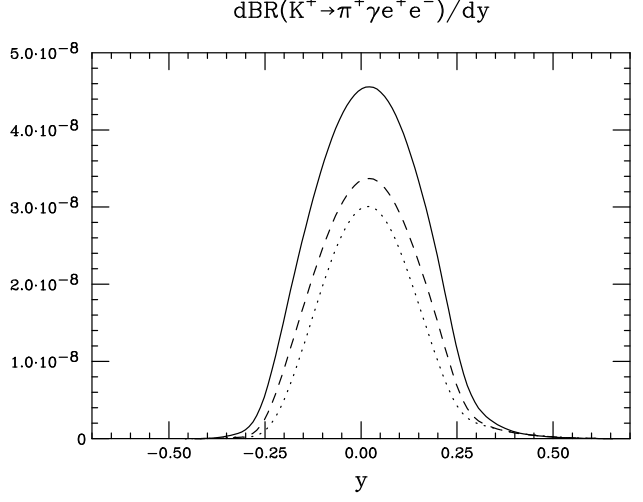
Figure 7: The differential branching ratio $dBR(K^+ \to \pi^+\gamma e^+e^-)/dy$ to order E^6 is plotted vs y for $\hat{c} = 1.8$ (solid line), $\hat{c} = 0$ (dashed line) and $\hat{c} = -2.3$ (dotted line).
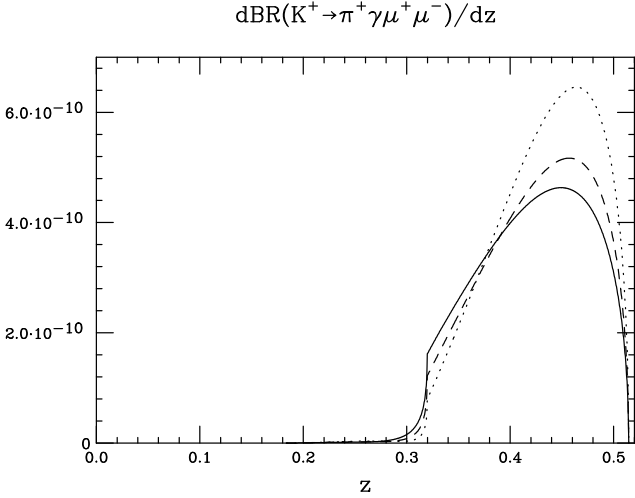
dBR(K⁺→π⁺γμ⁺μ⁻)/dz

dBR(K⁺→π⁺γμ⁺μ⁻)/dy

Figure 8: The differential branching ratio $dBR(K^+ \to \pi^+\gamma\mu^+\mu^-)/dz$ to order E^6 is plotted vs z for $\hat{c} = 1.8$ (solid line), $\hat{c} = 0$ (dashed line) and $\hat{c} = -2.3$ (dotted line).
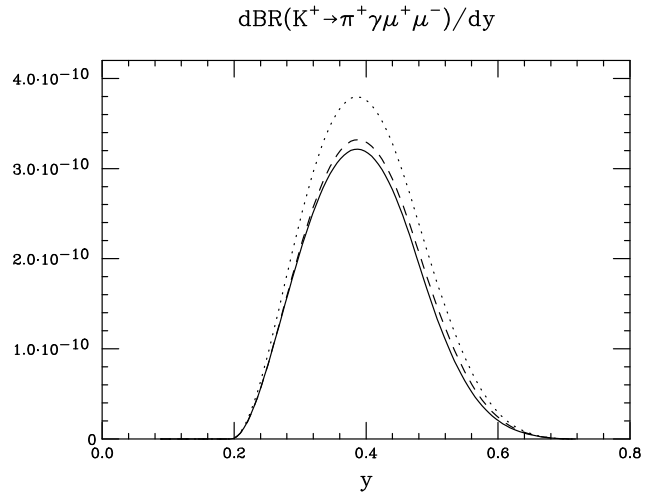
Figure 9: The differential branching ratio $dBR(K^+ \to \pi^+\gamma\mu^+\mu^-)/dy$ to order E^6 is plotted vs y for $\hat{c} = 1.8$ (solid line), $\hat{c} = 0$ (dashed line) and $\hat{c} = -2.3$ (dotted line).

Table 3: Results for $BR(K^+ \to \pi^+\gamma e^+e^-)$ at $\mathcal{O}(E^6)$ with the cuts defined by (34).

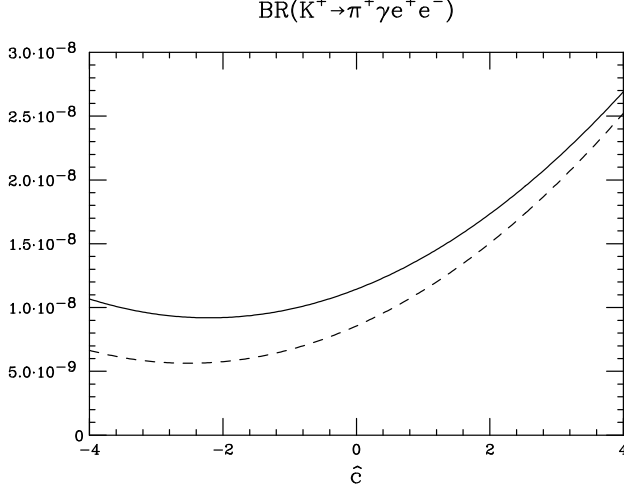|	$BR(K^+ \to \pi^+\gamma e^+e^-)$
$\hat{c} = 1.8$ (fit)	5.5×10^{-10}
$\hat{c} = 0$ (WDM)	4.8×10^{-10}
$\hat{c} = -2.3$ (FM)	4.7×10^{-10}

BR(K⁺→π⁺γe⁺e⁻)

Figure 10: The branching ratio BR($K^+ \rightarrow \pi^+\gamma e^+e^-$) is plotted vs $\hat{c}$ at $\mathcal{O}(\mathrm{E}^4)$ (dashed line) and up to $\mathcal{O}(\mathrm{E}^6)$ (solid line).
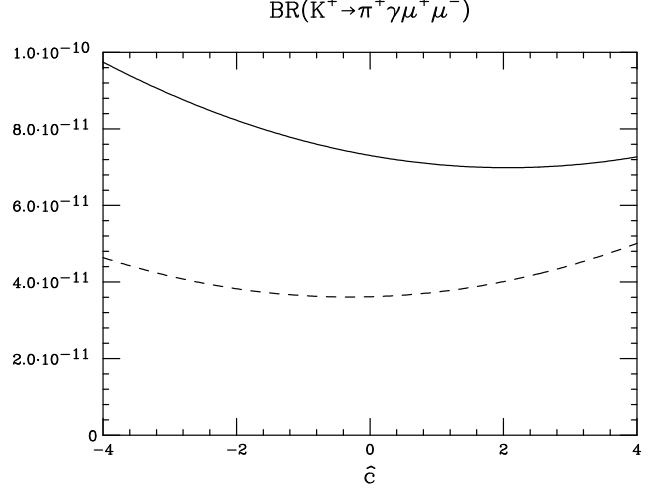
BR(K⁺→π⁺γμ⁺μ⁻)

Figure 11: The branching ratio BR($K^+ \rightarrow \pi^+\gamma\mu^+\mu^-$) is plotted vs $\hat{c}$ at $\mathcal{O}(\mathrm{E}^4)$ (dashed line) and up to $\mathcal{O}(\mathrm{E}^6)$ (solid line).
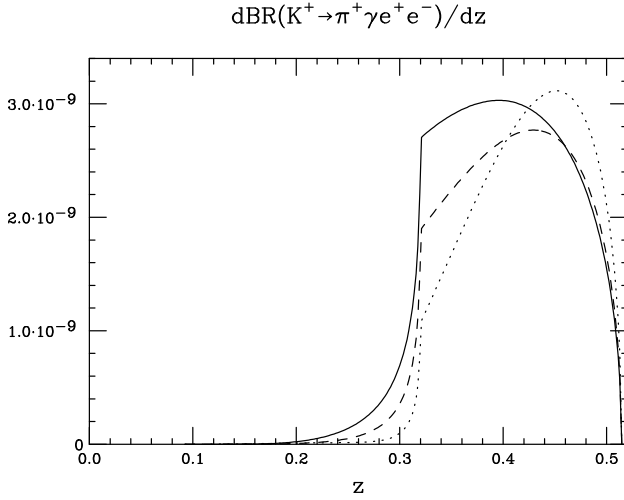
dBR(K⁺→π⁺γe⁺e⁻)/dz

Figure 12: The differential branching ratio dBR($K^+ \rightarrow \pi^+\gamma e^+e^-$)/dz to order E^6 is plotted vs z for $\hat{c} = 1.8$ (solid line), $\hat{c} = 0$ (dashed line) and $\hat{c} = -2.3$ (dotted line) with the cuts defined by the inequalities (34).
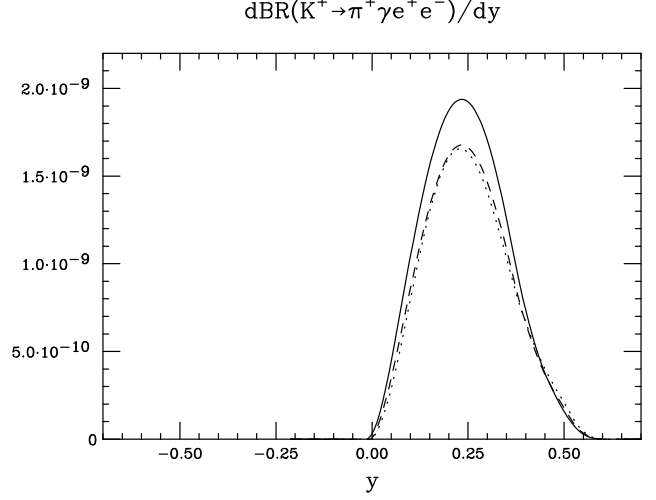
dBR(K⁺→π⁺γe⁺e⁻)/dy

Figure 13: Same as in Fig. 12 for the differential branching ratio dBR($K^+ \rightarrow \pi^+\gamma e^+e^-$)/dy vs y.

11

V. Conclusions

We have computed the unitarity corrections at one loop in ChPT for the processes $K^+ \to \pi^+ \gamma e^+ e^-$ and $K^+ \to \pi^+ \gamma \mu^+ \mu^-$, allowing us to present predictions for their total and differential branching ratios.

As expected, the muonic rate is significantly smaller than in the corresponding electronic mode, analogously to the cases studied in Refs. [3] and [4]. This is of course due to the more limited phase space, as well as the fact that the photon propagator is further off shell in the muonic case. We again see that the more complete calculation presented above leads to a conspicuous enhancement over the purely order E^4 calculation presented first. The vector meson diagrams here are not expected to add a significant amount to the overall rates and have been omitted altogether. Their inclusion provided a consistent contribution to the K_L decays, leading to dramatic increases in the $\mathcal{O}(E^6)$ results. Therefore, in the computation presented in this paper the enhancement is expected to be somewhat smaller.

The results for the differential branching ratios follow a pattern recognizable in all the previous calculations for radiative rare kaon decays: A large peak is visible above the two-pion threshold in the z variable, with a tail extended to low z, and a slightly asymmetrical and structureless distribution in the y variable. Experimentally, the abundance of information supplied by the former plots makes them a preferred option (see for example [7]). This is true also if we reduce the phase space of integration performing experimental cuts.

We also note that comparing Figs. 10 and 11, one sees that the dependence on $\hat{c}$ is markedly higher when electrons, instead of muons, are present in the final state. This has important consequences if one tries to extract the value of $\hat{c}$ from the data.

Acknowledgments

Appendix: Relevant integrals

In this appendix we list the explicit expressions for the integrals used in the calculation of Sec. IV. We follow the notation of that section. For $s \le 4m_\pi^2$ and $k_1^2 \le 4m_\pi^2$ we have

$$
\begin{aligned}
I_1(1) \;=\; & \frac{1}{s - k_1^2} \left\{ -\frac{3}{2}\left(s - k_1^2\right) - m_\pi^2 \left[F(s) - F(k_1^2)\right] \right. \\
& \left. - \sqrt{4m_\pi^2 - k_1^2}\,\arctan\sqrt{\frac{k_1^2}{4m_\pi^2 - k_1^2}} + \sqrt{4m_\pi^2 - s}\,\arctan\sqrt{\frac{s}{4m_\pi^2 - s}} \right\},
\end{aligned}
$$

$$(A1)$$

$$
\begin{aligned}
I_1(z_1) \;=\; & \frac{1}{s - k_1^2}\left[-\frac{4s}{9} - \frac{(4m_\pi^2 - s)}{3\sqrt{s}}\sqrt{4m_\pi^2 - s}\,\arctan\sqrt{\frac{s}{4m_\pi^2 - s}} \right. \\
& \left. + \frac{4k_1^2}{9} + \frac{(4m_\pi^2 - k_1^2)}{3\sqrt{k_1^2}}\sqrt{4m_\pi^2 - k_1^2}\,\arctan\sqrt{\frac{k_1^2}{4m_\pi^2 - k_1^2}} \right],
\end{aligned}
$$

$$(A2)$$

$$
I_1(z_1^2) \;=\; \frac{1}{s - k_1^2}\left[-\frac{2s}{9} - \frac{(4m_\pi^2 - s)}{6\sqrt{s}}\sqrt{4m_\pi^2 - s}\,\arctan\sqrt{\frac{s}{4m_\pi^2 - s}} \right.
$$

$$+ \quad \frac{2k_1^2}{9} + \frac{(4m_\pi^2 - k_1^2)}{6\sqrt{k_1^2}}\sqrt{4m_\pi^2 - k_1^2}\arctan\sqrt{\frac{k_1^2}{4m_\pi^2 - k_1^2}} \Bigg], \tag{A3}$$

$$\begin{aligned}
I_1(z_2) =& \; -\frac{4}{9} + \frac{3m_\pi^2 + k_1^2}{6(s - k_1^2)} + \frac{m_\pi^2}{3s} + \frac{(-4m_\pi^4 + 5m_\pi^2 s - s^2)}{3s\sqrt{s}\sqrt{4m_\pi^2 - s}}\arctan\sqrt{\frac{s}{4m_\pi^2 - s}} \\[2mm]
& - \; \frac{m_\pi^4}{2(s - k_1^2)^2}\left[2\frac{\sqrt{4m_\pi^2 - s}}{m_\pi^2}\arctan\sqrt{\frac{s}{4m_\pi^2 - s}} - \frac{s}{m_\pi^2} \right. \\[2mm]
& + \; 2\frac{\sqrt{4m_\pi^2 - k_1^2}}{m_\pi^2}\arctan\sqrt{\frac{k_1^2}{4m_\pi^2 - k_1^2}} + \frac{k}{m_\pi^2} \Bigg] \\[2mm]
& - \; \frac{k_1^4}{3(s - k_1^2)^2}\left[\frac{m_\pi^2}{s} + \frac{(-4m_\pi^4 + 5m_\pi^2 s - s^2)}{s\sqrt{s}\sqrt{4m_\pi^2 - s}}\arctan\sqrt{\frac{s}{4m_\pi^2 - s}} - \frac{m_\pi^2}{k_1^2} \right. \\[2mm]
& + \; \frac{(-4m_\pi^4 + 5m_\pi^2 k_2^2 - k_1^4)}{k_1^2\sqrt{k_1^2}\sqrt{4m_\pi^2 - k_1^2}}\arctan\sqrt{\frac{k_1^2}{4m_\pi^2 - k_1^2}} \Bigg] \\[2mm]
& + \; \frac{m_\pi^2 k_1^2}{(s - k_1^2)^2}\left[F(s) - F(k_1^2) \right] - \frac{2m_\pi^2 k_1^2}{(s - k_1^2)^2}\left[\frac{\sqrt{4m_\pi^2 - s}}{\sqrt{s}}\arctan\sqrt{\frac{s}{4m_\pi^2 - s}} \right. \\[2mm]
& - \; \frac{\sqrt{4m_\pi^2 - k_1^2}}{\sqrt{k_1^2}}\arctan\sqrt{\frac{k_1^2}{4m_\pi^2 - k_1^2}} \Bigg], \tag{A4}
\end{aligned}$$

$$\begin{aligned}
I_1(z_2^2) =& \; -\frac{2}{9} + \frac{m_\pi^2}{4(s - k_1^2)} + \frac{k_1^2}{24(s - k_1^2)} + \frac{1}{3(s - k_1^2)^2}\left(m_\pi^4 - 3m_\pi^2 k_1^2 - \frac{k_1^4}{4} \right) \\[2mm]
& + \; \frac{m_\pi^2}{3s} - \frac{(8m_\pi^4 - 6m_\pi^2 s + s^2)}{6s\sqrt{s}\sqrt{4m_\pi^2 - s}}\arctan\sqrt{\frac{s}{4m_\pi^2 - s}} \\[2mm]
& - \; \frac{m_\pi^6}{3(s - k_1^2)^3}\left[\frac{s}{m_\pi^2} + \frac{s\sqrt{s}\sqrt{4m_\pi^2 - s}}{m_\pi^4}\arctan\sqrt{\frac{s}{4m_\pi^2 - s}} \right. \\[2mm]
& - \; \frac{k_1^2}{m_\pi^2} - \frac{k_1^2\sqrt{k_1^2}\sqrt{4m_\pi^2 - k_1^2}}{m_\pi^4}\arctan\sqrt{\frac{k_1^2}{4m_\pi^2 - k_1^2}} \Bigg] \\[2mm]
& + \; \frac{k_1^6}{3(s - k_1^2)^3}\left[\frac{m_\pi^2}{s} - \frac{(8m_\pi^4 - 6m_\pi^2 s + s^2)}{2s\sqrt{s}\sqrt{4m_\pi^2 - s}}\arctan\sqrt{\frac{s}{4m_\pi^2 - s}} \right. \\[2mm]
& - \; \frac{m_\pi^2}{k_1^2} + \frac{(8m_\pi^4 - 6m_\pi^2 k_1^2 + k_1^4)}{2k_1^2\sqrt{k_1^2}\sqrt{4m_\pi^2 - k_1^2}}\arctan\sqrt{\frac{k_1^2}{4m_\pi^2 - k_1^2}} \Bigg] \\[2mm]
& + \; \frac{m_\pi^4 k_1^2}{(s - k_1^2)^3}\left[-\frac{s}{m_\pi^2} + \frac{2\sqrt{4m_\pi^2 - s}\sqrt{s}}{m_\pi^2}\arctan\sqrt{\frac{s}{4m_\pi^2 - s}} \right. \\[2mm]
& + \; \frac{k_1^2}{m_\pi^2} - \frac{2\sqrt{4m_\pi^2 - k_1^2}\sqrt{k_1^2}}{m_\pi^2}\arctan\sqrt{\frac{k_1^2}{4m_\pi^2 - k_1^2}} - F(s) + F(k_1^2) \Bigg]
\end{aligned}$$

$$- \frac{m_\pi^2 k_1^4}{(s-k_1^2)^3} \left[F(s) - \frac{3\sqrt{4m_\pi^2 - s}}{\sqrt{s}} \arctan\sqrt{\frac{s}{4m_\pi^2 - s}} \right.$$

$$- \left. F(k_1^2) + \frac{3\sqrt{4m_\pi^2 - k_1^2}}{\sqrt{k_1^2}} \arctan\sqrt{\frac{k_1^2}{4m_\pi^2 - k_1^2}} \right], \tag{A5}$$

$$
\begin{aligned}
I_1(z_1 z_2) =\ & -\frac{13}{144} + \frac{(-6m_\pi^2 + k_1^2)}{24(s-k_1^2)} + \frac{(8m_\pi^4 + 2m_\pi^2 s - s^2)}{12s\sqrt{s}\sqrt{4m_\pi^2 - s}} \arctan\sqrt{\frac{s}{4m_\pi^2 - s}} \\
& + \frac{m_\pi^4}{2(s-k_1^2)^2} \left[F(k_1^2) - F(s) \right] \\
& - \frac{k_1^4}{2(s-k_1^2)^2} \left[-\frac{m_\pi^2}{3s} + \frac{(8m_\pi^4 + 2m_\pi^2 s - s^2)}{6s\sqrt{s}\sqrt{4m_\pi^2 - s}} \arctan\sqrt{\frac{s}{4m_\pi^2 - s}} \right. \\
& + \left. \frac{m_\pi^2}{3k_1^2} - \frac{(8m_\pi^4 + 2m_\pi^2 k_1^2 - k_1^4)}{6k_1^2\sqrt{k_1^2}\sqrt{4m_\pi^2 - k_1^2}} \arctan\sqrt{\frac{k_1^2}{4m_\pi^2 - k_1^2}} \right] \\
& + \frac{m_\pi^2 k_1^2}{(s-k_1^2)^2} \left[\frac{\sqrt{4m_\pi^2 - s}}{\sqrt{s}} \arctan\sqrt{\frac{s}{4m_\pi^2 - s}} \right. \\
& - \left. \frac{\sqrt{4m_\pi^2 - k_1^2}}{\sqrt{k_1^2}} \arctan\sqrt{\frac{k_1^2}{4m_\pi^2 - k_1^2}} \right], \tag{A6}
\end{aligned}
$$

$$
\begin{aligned}
\frac{I_2(z_1 z_2)}{m_K^2} =\ & -\frac{1}{2(s-k_1^2)} - \frac{m_\pi^2}{(s-k_1^2)^2} \left[F(s) - F(k_1^2) \right] \\
& + \frac{k_1^2}{(s-k_1^2)^2} \left[\frac{\sqrt{4m_\pi^2 - s}}{\sqrt{s}} \arctan\sqrt{\frac{s}{4m_\pi^2 - s}} \right. \\
& - \left. \frac{\sqrt{4m_\pi^2 - k_1^2}}{\sqrt{k_1^2}} \arctan\sqrt{\frac{k_1^2}{4m_\pi^2 - k_1^2}} \right], \tag{A7}
\end{aligned}
$$

$$
\begin{aligned}
\frac{I_2(z_1 z_2^2)}{m_K^2} =\ & -\frac{1}{6(s-k_1^2)} + \frac{1}{(s-k_1^2)^2} \left(\frac{k_1^2}{3} + m_\pi^2 \right) \\
& - \frac{m_\pi^2}{(s-k_1^2)^3} \left[2\sqrt{4m_\pi^2 - s}\sqrt{s} \arctan\sqrt{\frac{s}{4m_\pi^2 - s}} - s \right. \\
& - \left. 2\sqrt{4m_\pi^2 - k_1^2}\sqrt{k_1^2} \arctan\sqrt{\frac{k_1^2}{4m_\pi^2 - k_1^2}} + k_1^2 \right] \\
& - \frac{2k_1^4}{3(s-k_1^2)^3} \left[\frac{m_\pi^2}{s} + \frac{(-4m_\pi^4 + 5m_\pi^2 s - s^2)}{s\sqrt{s}\sqrt{4m_\pi^2 - s}} \arctan\sqrt{\frac{s}{4m_\pi^2 - s}} \right. \\
& - \left. \frac{m_\pi^2}{k_1^2} - \frac{(-4m_\pi^4 + 5m_\pi^2 k_2^2 - k_1^4)}{k_1^2\sqrt{k_1^2}\sqrt{4m_\pi^2 - k_1^2}} \arctan\sqrt{\frac{k_1^2}{4m_\pi^2 - k_1^2}} \right.
\end{aligned}
$$

14

$$+\quad \frac{2m_\pi^2 k_1^2}{(s-k_1^2)^3}\left[F(s) - F(k_1^2) - \frac{2\sqrt{4m_\pi^2 - s}}{\sqrt{s}}\arctan\sqrt{\frac{s}{4m_\pi^2 - s}}\right.$$

$$+\quad \left.\frac{2\sqrt{4m_\pi^2 - k_1^2}}{\sqrt{k_1^2}}\arctan\sqrt{\frac{k_1^2}{4m_\pi^2 - k_1^2}}\right], \tag{A8}$$

$$\begin{aligned}
\frac{I_2(z_1 z_2^3)}{m_K^2} &= -\frac{1}{12(s-k_1^2)} + \frac{1}{(s-k_1^2)^2}\left(\frac{6m_\pi^2 + k_1^2}{4}\right) \\
&\quad - \frac{1}{(s-k_1^2)^3}\left(\frac{4m_\pi^4 - 12m_\pi^2 k_1^2 - k_1^4}{4}\right) \\
&\quad - \frac{m_\pi^6}{(s-k_1^2)^4}\left[\frac{s}{m_\pi^2} - \frac{k_1^2}{m_\pi^2} + \frac{s\sqrt{s}\sqrt{4m_\pi^2 - s}}{m_\pi^4}\arctan\sqrt{\frac{s}{4m_\pi^2 - s}}\right. \\
&\quad - \left.\frac{k_1^2\sqrt{k_1^2}\sqrt{4m_\pi^2 - k_1^2}}{m_\pi^4}\arctan\sqrt{\frac{k_1^2}{4m_\pi^2 - k_1^2}} - \frac{s^2}{4m_\pi^4} + \frac{k_1^4}{4m_\pi^4}\right] \\
&\quad + \frac{k_1^6}{(s-k_1^2)^4}\left[\frac{m_\pi^2}{s} - \frac{(8m_\pi^4 - 6m_\pi^2 s + s^2)}{s\sqrt{s}\sqrt{4m_\pi^2 - s}}\arctan\sqrt{\frac{s}{4m_\pi^2 - s}}\right. \\
&\quad - \frac{m_\pi^2}{k_1^2} + \left.\frac{(8m_\pi^4 - 6m_\pi^2 k_1^2 + k_1^4)}{k_1^2\sqrt{k_1^2}\sqrt{4m_\pi^2 - k_1^2}}\arctan\sqrt{\frac{k_1^2}{4m_\pi^2 - k_1^2}}\right] \\
&\quad + \frac{3m_\pi^4 k_1^2}{(s-k_1^2)^4}\left[\frac{2\sqrt{4m_\pi^2 - s}\sqrt{s}}{m_\pi^2}\arctan\sqrt{\frac{s}{4m_\pi^2 - s}} - \frac{s}{m_\pi^2}\right. \\
&\quad + \frac{k_1^2}{m_\pi^2} - \left.\frac{2\sqrt{4m_\pi^2 - k_1^2}\sqrt{k_1^2}}{m_\pi^2}\arctan\sqrt{\frac{k_1^2}{4m_\pi^2 - k_1^2}} - F(s) + F(k_1^2)\right] \\
&\quad - \frac{3m_\pi^2 k_1^4}{(s-k_1^2)^4}\left[F(s) - \frac{3\sqrt{4m_\pi^2 - s}}{\sqrt{s}}\arctan\sqrt{\frac{s}{4m_\pi^2 - s}}\right. \\
&\quad - F(k_1^2) + \left.\frac{3\sqrt{4m_\pi^2 - k_1^2}}{\sqrt{k_1^2}}\arctan\sqrt{\frac{k_1^2}{4m_\pi^2 - k_1^2}}\right], \tag{A9}
\end{aligned}$$

$$\begin{aligned}
\frac{I_2(z_1^2 z_2)}{m_K^2} &= -\frac{1}{6(s-k_1^2)} + \frac{1}{(s-k_1^2)^2}\left[-\frac{4m_\pi^2}{3}\right. \\
&\quad - \frac{\sqrt{k_1^2}\sqrt{4m_\pi^2 - k_1^2}}{3}\arctan\sqrt{\frac{k_1^2}{4m_\pi^2 - k_1^2}} \\
&\quad + \left.\frac{4m_\pi^2}{3\sqrt{k_1^2}}\sqrt{4m_\pi^2 - k_1^2}\arctan\sqrt{\frac{k_1^2}{4m_\pi^2 - k_1^2}}\right] - \frac{1}{(s-k_1^2)^2}\left[-2m_\pi^2 + \frac{2k_1^2 m_\pi^2}{3s}\right. \\
&\quad - \left.\sqrt{4m_\pi^2 - s}\frac{(2k_1^2 m_\pi^2 + k_1^2 s - 6m_\pi^2 s)}{3s\sqrt{s}}\arctan\sqrt{\frac{s}{4m_\pi^2 - s}}\right], \tag{A10}
\end{aligned}$$

$$\frac{I_2(z_1^2 z_2^2)}{m_K^2} = -\frac{1}{24(s-k_1^2)} - \frac{1}{12(s-k_1^2)^2}(6m_\pi^2 - k_1^2) - \frac{m_\pi^4}{(s-k_1^2)^3}\left[F(s) - F(k_1^2)\right]$$

$$- \frac{k_1^4}{(s-k_1^2)^3}\left[-\frac{m_\pi^2}{3s} + \frac{(8m_\pi^4 + 2m_\pi^2 s - s^2)}{6s\sqrt{s}\sqrt{4m_\pi^2 - s}}\arctan\sqrt{\frac{s}{4m_\pi^2 - s}}\right.$$

$$+ \frac{m_\pi^2}{3k_1^2} - \frac{(8m_\pi^4 + 2m_\pi^2 k_1^2 - k_1^4)}{6k_1^2\sqrt{k_1^2}\sqrt{4m_\pi^2 - k_1^2}}\arctan\sqrt{\frac{k_1^2}{4m_\pi^2 - k_1^2}}\right]$$

$$+ \frac{2m_\pi^2 k_1^2}{(s-k_1^2)^3}\left[-\frac{\sqrt{4m_\pi^2 - k_1^2}}{\sqrt{k_1^2}}\arctan\sqrt{\frac{k_1^2}{4m_\pi^2 - k_1^2}}\right.$$

$$+ \left.\frac{\sqrt{4m_\pi^2 - s}}{\sqrt{s}}\arctan\sqrt{\frac{s}{4m_\pi^2 - s}}\right], \tag{A11}$$

$$\frac{I_2(z_1^3 z_2)}{m_K^2} = -\frac{1}{12(s-k_1^2)} + \frac{1}{2(s-k_1^2)^2}\left[-\frac{4m_\pi^2}{3}\right.$$

$$- \frac{\sqrt{k_1^2}\sqrt{4m_\pi^2 - k_1^2}}{3}\arctan\sqrt{\frac{k_1^2}{4m_\pi^2 - k_1^2}}$$

$$+ \left.\frac{4m_\pi^2}{3\sqrt{k_1^2}}\sqrt{4m_\pi^2 - k_1^2}\arctan\sqrt{\frac{k_1^2}{4m_\pi^2 - k_1^2}}\right] - \frac{1}{2(s-k_1^2)^2}\left[-2m_\pi^2 + \frac{2k_1^2 m_\pi^2}{3s}\right.$$

$$- \left.\sqrt{4m_\pi^2 - s}\frac{(2k_1^2 m_\pi^2 + k_1^2 s - 6m_\pi^2 s)}{3s\sqrt{s}}\arctan\sqrt{\frac{s}{4m_\pi^2 - s}}\right], \tag{A12}$$

$$I_3 m_K^2 = -\frac{13}{12}m_\pi^2 + \frac{13}{144}\left(s + k_1^2\right) - \frac{m_\pi^4}{2(s-k_1^2)}\left[F(s) - F(k_1^2)\right]$$

$$- \frac{k_1^4}{2(s-k_1^2)}\left[-\frac{(8m_\pi^4 + 2m_\pi^2 k_1^2 - k_1^4)}{6k_1^2\sqrt{k_1^2}\sqrt{4m_\pi^2 - k_1^2}}\arctan\sqrt{\frac{k_1^2}{4m_\pi^2 - k_1^2}}\right.$$

$$+ \left.\frac{(8m_\pi^4 + 2m_\pi^2 s - s^2)}{6s\sqrt{s}\sqrt{4m_\pi^2 - s}}\arctan\sqrt{\frac{s}{4m_\pi^2 - s}}\right]$$

$$+ \frac{k_1^2 m_\pi^2}{s-k_1^2}\left[-\frac{\sqrt{4m_\pi^2 - k_1^2}}{\sqrt{k_1^2}}\arctan\sqrt{\frac{k_1^2}{4m_\pi^2 - k_1^2}}\right.$$

$$+ \left.\frac{\sqrt{4m_\pi^2 - s}}{\sqrt{s}}\arctan\sqrt{\frac{s}{4m_\pi^2 - s}}\right]$$

$$- \sqrt{4m_\pi^2 - s}\frac{(2k_1^2 m_\pi^2 + k_1^2 s - 10m_\pi^2 s + s^2)}{12s\sqrt{s}}\arctan\sqrt{\frac{s}{4m_\pi^2 - s}}, \tag{A13}$$

$$I_4 m_K^2 = \frac{5k_1^2}{18} - \frac{4m_\pi^2}{3} + \frac{(4m_\pi^2 - k_1^2)\sqrt{4m_\pi^2 - k_1^2}}{3\sqrt{k_1^2}} \arctan\sqrt{\frac{k_1^2}{4m_\pi^2 - k_1^2}}, \tag{A14}$$

$$I_5 = -\frac{8}{9} + \frac{8m_\pi^2}{3k_1^2} - \frac{2(4m_\pi^2 - k_1^2)\sqrt{4m_\pi^2 - k_1^2}}{3k_1^2\sqrt{k_1^2}} \arctan\sqrt{\frac{k_1^2}{4m_\pi^2 - k_1^2}}. \tag{A15}$$

In the cases when $s > 4m_\pi^2$ or $k_1^2 > 4m_\pi^2$, we have to perform the substitutions

$$\arctan\sqrt{\frac{s}{4m_\pi^2 - s}} \rightarrow -\frac{1}{2i}\left[\log\left(\frac{1 - \sqrt{1 - 4m_\pi^2/s}}{1 + \sqrt{1 - 4m_\pi^2/s}}\right) + i\pi\right],$$

$$\arctan\sqrt{\frac{k_1^2}{4m_\pi^2 - k_1^2}} \rightarrow -\frac{1}{2i}\left[\log\left(\frac{1 - \sqrt{1 - 4m_\pi^2/k_1^2}}{1 + \sqrt{1 - 4m_\pi^2/k_1^2}}\right) + i\pi\right], \tag{A16}$$

and

$$\sqrt{4m_\pi^2 - s} \rightarrow i\sqrt{s - 4m_\pi^2},$$
$$\sqrt{4m_\pi^2 - k_1^2} \rightarrow i\sqrt{k_1^2 - 4m_\pi^2}, \tag{A17}$$

respectively, in formulas (A1)–(A15).

References

[1] S. Weinberg, Physica A **96**, 327 (1979); J. Gasser and H. Leutwyler, Ann. Phys. (N.Y.) **158**, 142 (1984); Nucl. Phys. **B250**, 465 (1985).

[2] G. D'Ambrosio, G. Ecker, G. Isidori and H. Neufeld, in *The Second DAΦNE Physics Handbook*, edited by L. Maiani, G. Pancheri and N. Paver, (LNF, Frascati, 1995), p. 265.

[3] J.F. Donoghue and F. Gabbiani, Phys. Rev. D **56**, 1605 (1997).

[4] J.F. Donoghue and F. Gabbiani, Phys. Rev. D **58**, 037504 (1998).

[5] G. D'Ambrosio, G. Ecker, G. Isidori and J. Portolés, J. High Energy Phys. **08**, 004 (1998).

[6] R. Ben-David, Nucl. Phys. B (Proc. Suppl.) **66** 473 (1998); S.H. Kettell, presented at the 25th SLAC Summer Institute on Particle Physics: Physics of Leptons, Stanford, California, 1997, hep-ex/9801016.

[7] D. Bryman, ICHEP98, TRIUMF, Vancouver, British Columbia, Canada, 1998; E. Cheu, *ibid.*

[8] J.F. Donoghue, B.R. Holstein and G. Valencia, Phys. Rev. D **35**, 2769 (1987); G. Ecker, A. Pich and E. de Rafael, Phys. Lett. B **189**, 363 (1987); L. Cappiello and G. D'Ambrosio, Nuovo Cimento **A 99**, 155 (1988); L.M. Sehgal, Phys. Rev. D **38**, 808 (1988); P. Ko and J. Rosner, *ibid.* **40**, 3775 (1989); J. Kambor and B.R. Holstein, *ibid.* **49**,2346 (1994).

[9] A.G. Cohen, G. Ecker and A. Pich, Phys. Lett. B **304**, 347 (1993).

[10] L. Cappiello, G. D'Ambrosio and M. Miragliuolo, Phys. Lett. B **298**, 423 (1993);

[11] J.F. Donoghue and F. Gabbiani, Phys. Rev. D **51**, 2187 (1995).

[12] G. D'Ambrosio and J. Portolés, Phys. Lett. B **386**, 403 (1996).

[13] G. D'Ambrosio and J. Portolés, Nucl. Phys. **B492**, 417 (1997).

[14] T. Morozumi and H. Iwasaki, Prog. Theor. Phys. **82**, 371 (1989); J. Flynn and L. Randall, Phys. Lett. B **216**, 221 (1989); L.M. Sehgal, Phys. Rev. D **41**, 161 (1990); P. Ko, *ibid.* **41**, 1531 (1990); J. Bijnens, S. Dawson and G. Valencia, *ibid.* **44**, 3555 (1991); T. Hambye, Int. J. Mod. Phys. A **7**, 135 (1992); P. Heiliger and L.M. Sehgal, Phys. Rev. D **47**, 4920 (1993).

[15] G. D'Ambrosio and G. Isidori, Z. Phys. C **65**, 649 (1995).

[16] G. Ecker, A. Pich and E. de Rafael, Nucl. Phys. **B291**, 692 (1987).

[17] G. Ecker, A. Pich and E. de Rafael, Nucl. Phys. **B303**, 665 (1988).

[18] M. Kobayashi and T. Maskawa, Prog. Theor. Phys. **49**, 652 (1973).

[19] J. Kambor, J. Missimer and D. Wyler, Nucl. Phys. **B346**, 17 (1990).

[20] G. Ecker, A. Pich and E. de Rafael, Phys. Lett. B **237**, 481 (1990).

[21] G. Ecker, J Kambor and D. Wyler, Nucl. Phys. **B394**, 101 (1993); G. Isidori and A. Pugliese, *ibid.* **385**, 437 (1992); C. Bruno and J. Prades, Z. Phys. C **57**, 585 (1993).

[22] A. Pich and E. de Rafael, Nucl. Phys. **B358**, 311 (1991).

[23] P. Kitching *et al.*, Phys. Rev. Lett. **79**, 4079 (1997).

[24] Particle Data Group, C. Caso *et al.*, Eur. Phys. J. C **3**, 1 (1998).

[25] J. Wess and B. Zumino, Phys. Lett. **37B**, 95 (1971); E. Witten, Nucl. Phys. **B223**, 422 (1983).

[26] J.F. Donoghue, E. Golowich and B.R. Holstein, Phys. Rev. D **30**, 587 (1984).

[27] G. D'Ambrosio and G. Isidori, Int. J. Mod. Phys. A **13**, 1 (1998).

[28] J. Kambor, J. Missimer and D. Wyler, Phys. Lett. B **261**, 496 (1991); L. Maiani and N. Paver, in *The Second DAΦNE Physics Handbook*, edited by L. Maiani, G. Pancheri and N. Paver, (LNF, Frascati, 1995), p. 239.

[29] J.F. Donoghue and B.R. Holstein, Phys. Rev. Lett. **68**, 1818 (1992).

[30] C. Zemach, Phys. Rev. **133**, B1201 (1964); T.J. Devlin and J.O. Dickey, Rev. Mod. Phys. **51**, 237 (1979).

[31] A. Poblaguev (private communications).